coatings

MDPI

Article

Microstructure and Oxidation Resistance of a Si Doped Platinum Modified Aluminide Coating Deposited on a Single Crystal Superalloy

Qixiang Fan [1,*], Haojun Yu [2,*], Tiegang Wang [1] and Yanmei Liu [1]

[1] Tianjin Key Laboratory of High Speed Cutting and Precision Machining, Tianjin University of Technology and Education, Tianjin 300222, China; tgwang@tute.edu.cn (T.W.); ymliu@tute.edu.cn (Y.L.)
[2] Institute of Metal Research, Chinese Academy of Sciences, Shenyang 110016, China
* Correspondence: qxfan@tute.edu.cn (Q.F.); hjyu11s@imr.ac.cn (H.Y.); Tel.: +86-22-8818-1083 (Q.F.); +86-24-8397-8032 (H.Y.)

Received: 12 June 2018; Accepted: 25 July 2018; Published: 27 July 2018

Abstract: A Si doped Pt modified aluminide coating was prepared by electroplating and the chemical vapour deposition method. The microstructure and oxidation resistance of the coating were studied, with a single Pt modified aluminide coating as a reference. The results showed that the Si doped Pt modified aluminide coating consisted of singular β-(Ni, Pt)Al phase, and no $PtAl_2$ phase was detected, which might be due to the fact that the addition of Si retarded the formation of $PtAl_2$ phase in the outer layer. Si was dissolved in the β-(Ni, Pt)Al phase in the outer layer and might form silicide with refractory elements in the inter-diffusion zone. The Si doped Pt modified aluminide coating possesses a better oxidation resistance than the Pt modified aluminide coating since Si could promote the formation of α-Al_2O_3 and inhibit the diffusion of the refractory elements, reducing the formation of detrimental volatile phase.

Keywords: metal coatings; superalloy; platinum; SEM; oxidation

1. Introduction

With increasing intense energy supplies and more concerns on environmental protection, researchers are devoted to promoting the efficiency of gas turbine engines and the combustion ratio of fuels, which demands a higher turbine inlet temperature. This results in an increased service temperature and enhanced high temperature oxidation of the blades. Thus, it is necessary to develop novel protective coatings which can serve at elevated temperatures to meet the more demanding requirements for blade materials [1]. The properties of protective coating primarily rely on the formation of a stable, continuous, and adherent layer of α-Al_2O_3 scale, which delays the inward diffusion of the oxidative elements and protects the substrate from further oxidation. The element Pt has been demonstrated to be effective in promoting the formation, as well as the stability, of the α-Al_2O_3 scale since it could accelerate the outward diffusion rate of Al [2]. Besides, it could inhibit the void growth at the scale-metal interface, which is beneficial to improving the adhesion strength between the alumina layer and coating [3–5]. Moreover, Pt could reduce the outward diffusion of the refractory elements like W and Mo in the substrate [6]. Thus, the Pt modified aluminide coating possesses much better properties than the simple aluminide coating, and is extensively used in turbine engines.

Nowadays, many researchers try to add other elements into the Pt modified aluminide coating to take advantage of the synergistic effects of multiple alloying elements in order to further enhance the comprehensive properties of the coating. Zhou et al. [7] prepared a Pt/Dy co-doped aluminide coating and found that the coupled effects of Pt/Dy co-doping led to a lower oxidation rate, less scale rumpling, and improved scale adherence compared to the single Pt or Dy doping. Some other researchers revealed

that the addition of Hf into a single-phase Pt modified aluminide coating could lower the oxidation rate and decrease the oxide scale rumpling tendency, as Hf doped in the β-(Ni, Pt)Al coating could delay the transitional oxidation period from metastable alumina to a stable one and postpone the phase degradation from β-NiAl to γ-Ni/γ′-Ni_3Al [8]. Other beneficial elements such as Ru, Zr, etc. applied to the Pt modified aluminide coating have also been studied, and it is reported that the multi-element doped coatings possessed a better resistance to rumpling than the single Pt modified aluminide coating [9–11].

Among the modifying elements, Si has been reported to be effective in improving the oxidation resistance, hot corrosion performance, and thermal shock resistance of the aluminide coatings [12,13]. Because of these benefits, Si has been co-doped into the aluminide coatings with Dy or Co, and experimental results revealed that the oxidation resistance, as well as the hot corrosion resistance, of the coatings were enhanced greatly because Si could distribute at the grain boundaries to suppress the formation of metastable Al_2O_3 and increase the activity of Al, which was helpful in promoting the selective oxidation of α-Al_2O_3 scale [1,14–16]. Si has also been added into a binary-phase Pt modified aluminide coating by the slurry-aluminizing process and the microstructure evolution of the Si/Pt co-modified aluminide coating was studied [17]. However, no further research on the Si doped Pt modified aluminide coating has been reported up to now. In this paper, to figure out the effect of Si on the microstructure and oxidation resistance of the Pt modified aluminide coating, a kind of Si doped Pt modified aluminide coating was prepared by a two-step process: first electroplating a layer of Pt and then depositing Al and Si simultaneously using the chemical vapour deposition process. The microstructure and phase evolution before and after oxidation were studied in detail.

2. Materials and Methods

A single crystalline Ni-based superalloy with chemical compositions of 63.15 wt.% Ni-7.5 wt.% Co-7.0 wt.% Cr-1.5 wt.% Mo-5.0 wt.% W-6.2 wt.% Al-6.5 wt.% Ta-3.0 wt.% Re-0.15 wt.% Hf was used as the substrate, which was cut into round coupons with a radius of 15 mm. Prior to being sandblasted by alumina balls, the samples were ground by 150 #, 400 #, and 800 # SiC papers successively to eliminate the rust and deep scratches on the surface. Then, the samples were ultrasonically cleaned within acetone, ethanol, and deionized water. After being dried, the samples were put in a Q-salt electroplating bath to deposit a layer of Pt coating with a thickness of 2–4 μm. The samples with Pt coatings were treated by vacuum annealing at 1080 °C for 2 h to make the formation of the Pt modified aluminide coating easier. Then, the samples were hung over a pack power mixture made up of Al source, Si source, inert filler Al_2O_3, and activator NH_4F in a furnace chamber. The NH_4F decomposes into NH_3 and HF at high temperature, the HF reacted with Al as well as Si sources, and the active fluorides of Al (AlF_x, x = 1–3) and Si (SiF_y, y = 1–4) were formed to deposit Al and Si on the substrate. The Si doped Pt modified aluminide coating is abbreviated as a PtSiAl coating in this paper. As a reference coating, the Pt modified aluminide coating (abbreviated as PtAl coating) was prepared using the pack powder mixture composed of Al source, inert filler Al_2O_3, and activator NH_4F. The deposition temperature of these two coatings was 1080 °C and the duration time was 4 h.

Isothermal oxidation behavior of the PtAl and PtSiAl coatings was performed in static air atmosphere at 1100 °C for 320 h. To obtain the mass gain of the coatings during the oxidation process, the specimens were placed in alumina crucibles which were dried at 1200 °C for 24 h to exclude the interior volatile impurities and kept at a constant weight. The crucibles were taken out of the furnace and cooled down to room temperature at intervals. To count the mass of the spalled oxide, the mass gains of the specimens together with crucibles were weighed by an electronic balance with a sensitivity of about 10^{-4} g. For each test, three parallel samples were used to acquire the mean value of the mass gain, and each sample was measured five times to obtain the average value.

The major phases of the coatings before and after the oxidation tests were characterized by a D/MAX-RA X-ray diffractometer (XRD, X' Pert PRD, PANalytical, EA Almelo, The Netherlands) with monochromatic Cu Kα (λ = 0.154056 nm) radiation operated at 50 kV and 300 mA. The scanning

scope ranged from 10° to 90° with a 0.02° step size and 5°/min scanning speed. Cross-sectional microstructure and chemical compositions of the coatings and oxidation products were observed by a scanning electronic microscope (SEM, Inspect F, FEI, Hillsboro, OR, USA) equipped with an energy disperse spectroscope (EDS, Swift-ED, Oxford, UK) at 25 keV. INCA software (7.0, ETAS, Oxford, UK) was also used to analyze the compositions of the coatings. To avoid the destruction of the oxidation scale during the cross-sectional sample preparation process, a layer of Ni-P was electroless-plated on the surface of the coatings after oxidation. The compositions of the electroless plating bath were reported in a previous paper [18]. The area fraction of γ′-Ni_3Al phase in the outer layer after oxidation was measured by the Image J software (2x, National Institutes of Health, Bethesda, MD, USA). The detail measuring method was described in another paper [19].

3. Results and Discussion

3.1. Microstructures of the Coatings

Figure 1 shows the X-ray diffraction patterns of the PtAl and PtSiAl coatings. It can be seen that the main phase of the PtAl coating is the β-(Ni, Pt)Al phase with a minor diffraction peak as the ξ-$PtAl_2$ phase emerged. As for the Si doped Pt modified aluminide coating, only the β-(Ni, Pt)Al phase is detected, indicating that the addition of Si into the Pt modified aluminide coating could hinder the formation of the $PtAl_2$ phase during the silico-aluminizing process. It is worth noting that the diffraction peaks of the β-(Ni, Pt)Al phase in the two coatings shift to lower angles compared with those of the β-NiAl phase (PDF 44-1188, $a = b = c = 2.888$ Å). This is due to the fact that the radius atom of the Pt element is larger than that of the Ni element and it enlarged the lattice constant of the β-NiAl phase when Pt atoms replaced Ni sites in the NiAl crystal lattice [20]. The lattice constant of β-(Ni, Pt)Al phase increases to 2.904 Å, calculated by Jade software (6.0).

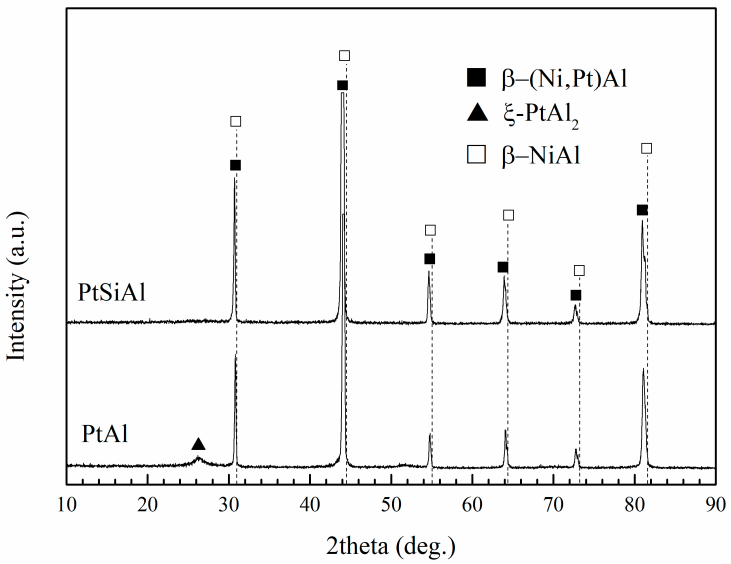

Figure 1. XRD patterns of the PtAl and PtSiAl coatings.

The surface morphologies of the PtAl and PtSiAl coatings are presented in Figure 2. As can be seen in Figure 2a, the surface of the PtAl coating displays two distinct structures (area A and area B). Area A is dense and smooth, while in area B, there are many black dots, which are demonstrated to be holes in a higher magnification image. In Figure 2b, the surface of the PtSiAl coating is dense with some ridges between the particles. The number of holes in the PtSiAl coating is much less than that in the PtAl coating, which reveals that the addition of Si into the Pt modified aluminide coating could diminish holes on the coating surface and make the coating denser.

The cross-sectional morphologies of the PtAl and PtSiAl coatings are shown in Figure 3. Both of the PtAl and PtSiAl coatings bear a two-layer structure. The outer layer is primarily composed of the β-(Ni, Pt)Al phase. Since the diffraction peaks of the $PtAl_2$ phase are very weakly detected by XRD, it is not distinct in the outer layer of the PtAl coating. The inner layer is the diffusion layer which consists of the β-(Ni, Pt)Al phase and some Cr(W) bright white phases, which form due to the phase transformation from the γ-Ni into the β-(Ni, Pt)Al phase and the refractory elements, e.g., Cr, W, etc. possess a higher solubility in the γ-Ni than those in the β-(Ni, Pt)Al phase. The black dots at the interface between the inner layer and outer layer are alumina particles left during the sand blasting process, which reveals that this interface is the original substrate surface and both of the two coatings form primarily through the outward diffusion of the Ni element. The average compositions in the outer layers of the PtAl and PtSiAl coatings are 46.2Al-1.9Cr-4.5Co-43.5Ni-3.9Pt (at.%) and 43.6Al-2.3Cr-4.1Co-45.6Ni-3.9Pt-0.7Si (at.%), respectively. It can be seen that the Al content in the PtSiAl coating is lower than that in the PtAl coating, while the Ni content is higher in the PtSiAl coating. The thicknesses of the PtAl and PtSiAl coatings are about 54 μm and 55 μm, respectively.

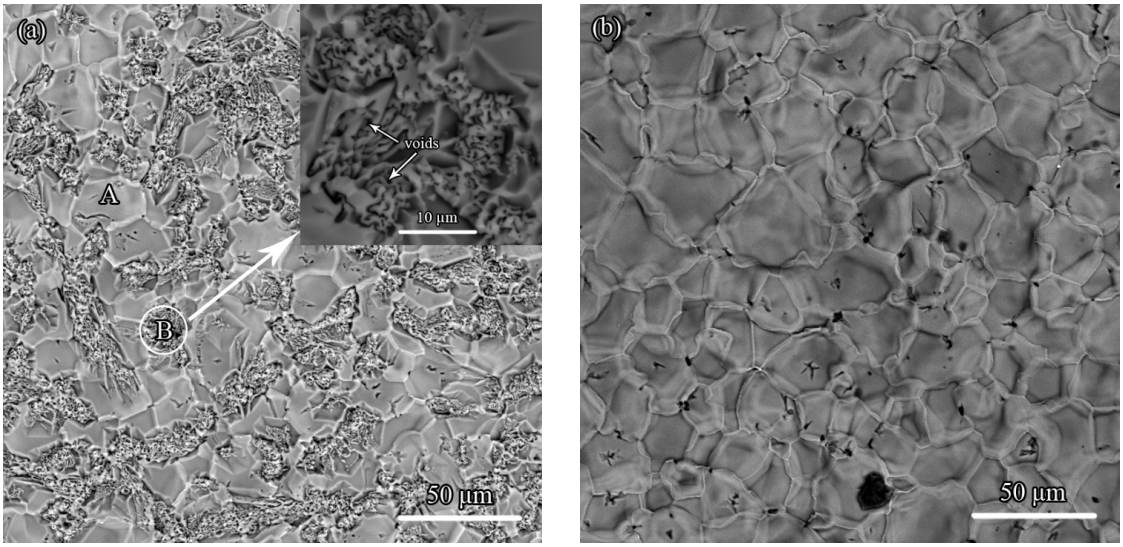

Figure 2. Surface morphologies of the coatings before oxidation: (**a**) PtAl and (**b**) PtSiAl.

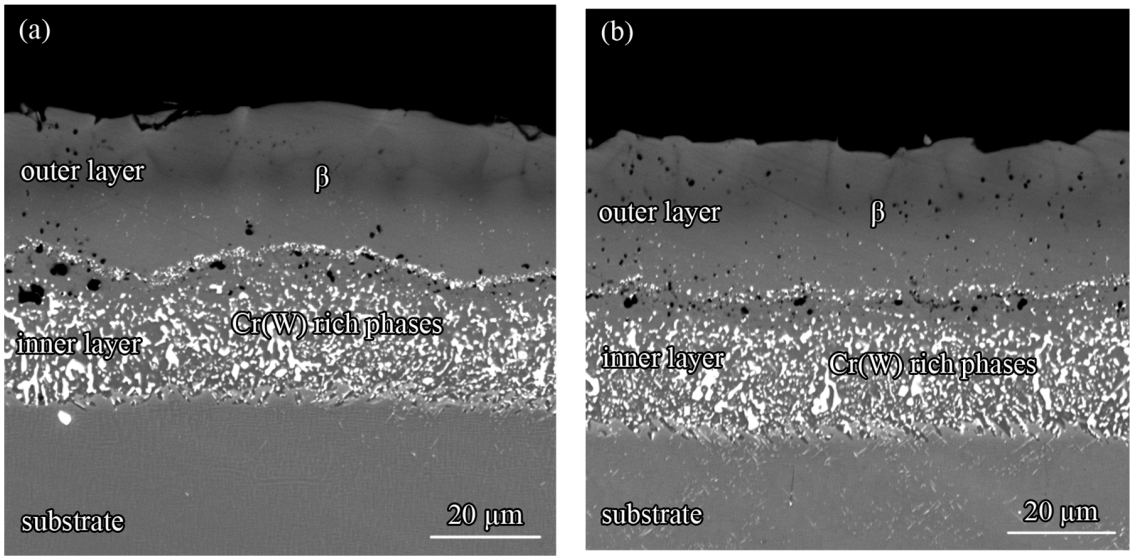

Figure 3. Cross-sectional morphologies of the coatings before oxidation: (**a**) PtAl and (**b**) PtSiAl.

3.2. Oxidation Kinetic Curves

Figure 4 shows the kinetic curves of the PtAl and PtSiAl coatings after isothermal oxidation at 1100 °C for 320 h. At the initial 30 h, the mass gain of the two coatings increases dramatically, since rapid oxidation of the coatings happens once the samples are exposed to the high temperature environment. The mass gain of the PtAl coating is lower than that of the PtSiAl coating at this stage. After that, the oxidation rate of the two coatings decreases dramatically and the mass gain reaches a stable stage, as a continuous and dense alumina layer is formed on the coating surface which could delay the inward diffusion of the oxidative elements and protect the substrate from further oxidation. The maximum mass gains of the PtAl and PtSiAl coatings are about 1.37 mg/cm^2 and 1.26 mg/cm^2, respectively, demonstrating that the PtSiAl coating is more mildly oxidized than the PtAl coating when the adherent alumina scale is formed on the surface at 1100 °C.

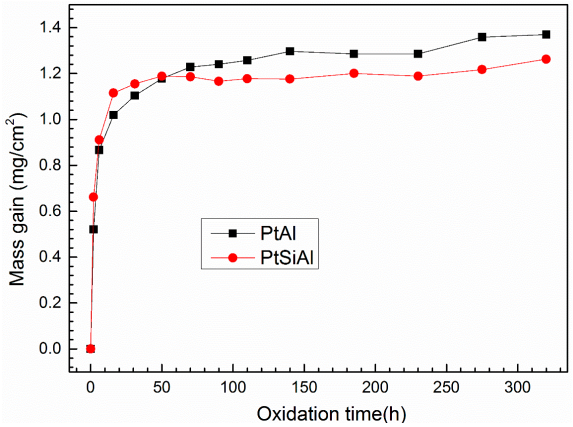

Figure 4. Kinetic curves of the PtAl and PtSiAl coatings after isothermal oxidation at 1100 °C for 320 h.

3.3. Oxidation Products

The X-ray patterns of the PtAl and PtSiAl coatings after isothermal oxidation at 1100 °C for 320 h are presented in Figure 5. As the oxidation proceeds to 320 h, the main phase of the two coatings transits from the β-(Ni, Pt)Al to the γ′-Ni_3Al phase due to the large depletion of the beneficial element Al. The Al_2O_3 phase is detected and no diffraction peaks of other oxides emerged, because both of the two coatings contain a high content of Al in the outer layer and the Gibbs free energy of Al_2O_3 is much lower than that of other oxides like NiO and Cr_2O_3, resulting in the preferential oxidation of Al after an instant oxidation stage. Note that the $PtAl_2$ phase diminishes in the PtAl coating since the $PtAl_2$ phase is metastable and it would transit to the β-(Ni, Pt)Al phase at high temperature [20,21].

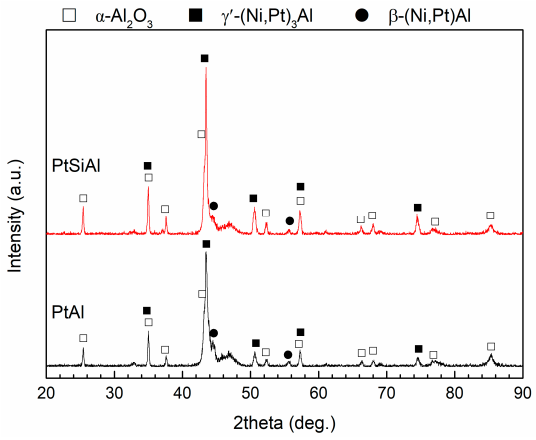

Figure 5. XRD patterns of the PtAl and PtSiAl coatings after isothermal oxidation at 1100 °C for 320 h.

The cross-sectional morphologies of the PtAl and PtSiAl coatings after oxidation at 1100 °C for 2 h are presented in Figure 6. A very thin layer of Al_2O_3 is formed on the surface of the PtAl and PtSiAl coatings. The outer layer is mainly composed of β-(Ni, Pt)Al phase and the γ′-Ni_3Al phase is not visible.

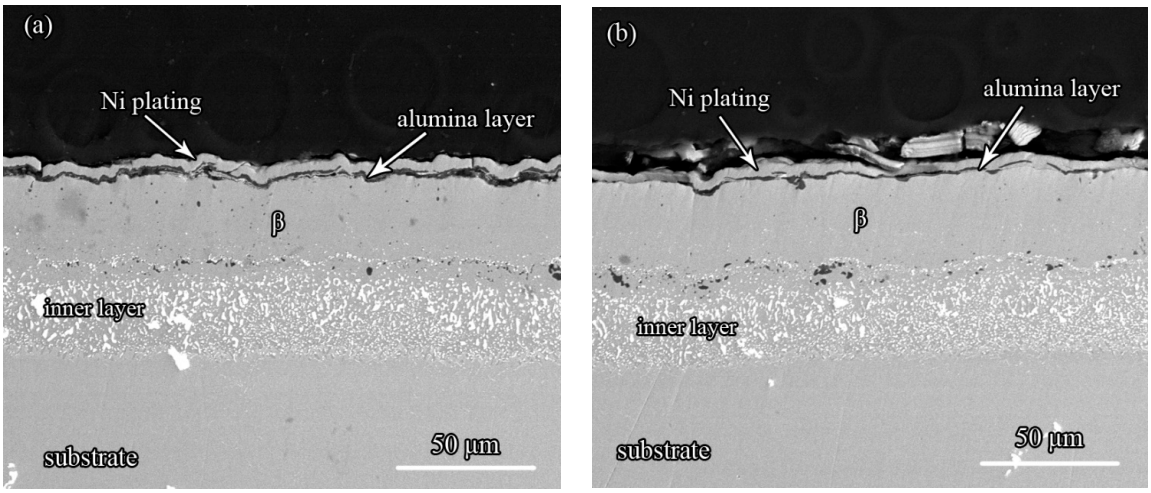

Figure 6. Cross-sectional morphologies of the coatings after oxidation at 1100 °C for 2 h: (**a**) PtAl and (**b**) PtSiAl.

The surface and cross-sectional morphologies of the PtAl and PtSiAl coatings after oxidation at 1100 °C for 320 h are presented in Figures 7 and 8, respectively. As can be seen in Figure 7, the surface of the two coatings is uneven. Moreover, spallation as well as cracking occur on the surface. The average chemical compositions of area A (black grey zone) on the PtAl and PtSiAl coatings in Figure 7a,b are 50.2O-46.4Al-1.6Ni-1.9W (at.%) and 57.7O-39.9Al-1.2Ni-1.2W (at.%), respectively, indicating that the surface of the two coatings is mainly made up of the α-Al_2O_3 phase, which is consistent with the XRD patterns shown in Figure 5. As for area B (bright white zone) of the two coatings, the average compositions are 19.3O-18.2Al-3.0Cr-5.3Co-48.7Ni-3.0W-2.4Pt-0.2Hf (at.%) and 12.4O-22.5Al-4.9Si-3.0Cr-4.1Co-40.6Ni-2.5Pt-0.1Hf (at.%), respectively. The Ni content in the white space is high because the spallation of the alumina layer leads to the exposure of the coating underneath. During the whole oxidation process, the alumina layer grows gradually, resulting in the generation of large growth stress, and the phase transition from θ/γ-Al_2O_3 to stable α-Al_2O_3 also induces internal stress in the alumina layer. Moreover, thermal stress is generated during the heating and cooling process. When the total internal stress is too high, the alumina scale first cracks and then peels off from the surface. The crack and spallation of the alumina layer could provide diffusion paths for the oxidative elements and speed up the degeneration of the coatings. When the Al content in the coating is high enough to sustain the exclusive oxidation of α-Al_2O_3, a new alumina layer is formed in the spallation area once the coating is exposed to the oxidative environment again. While, if the Al content is not high enough to sustain the selective oxidation of α-Al_2O_3, other oxides are formed. The mixed oxides are porous and not protective, and on the contrary, accelerate the oxidation of the substrate, meaning that the coating loses efficacy. As can be seen in Figure 5, no other oxides are detected by XRD, and a NiAl phase remains in both of the PtAl and PtSiAl coatings, demonstrating that the two coatings are still protective.

As shown in Figure 8, the alumina layer on the surface of the PtAl and PtSiAl coatings becomes thicker than that on the coatings oxidized for 2 h (in Figure 6), since the alumina layer grows gradually as the oxidation proceeds. It is obvious that the alumina layer formed on the PtAl coating is thicker than that formed on the PtSiAl coating. Amounts of β-(Ni, Pt)Al phase in the outer layer are transformed into the γ′-Ni_3Al phase to perform the exclusive oxidation of Al. The relative area fractions of the

γ′-Ni_3Al phase in the outer layer of the PtAl and PtSiAl coating are 12.9% and 11.7%, respectively, indicating that more β-(Ni, Pt)Al phase has been consumed in the PtAl coating. As has been reported, compared with the outward diffusion of Al element to form the protective alumina scale, the mutual diffusion between the coating and substrate plays an even more important role in the degeneration of the coatings at the temperature of 1100 °C [18]. Since the elements like Ni and W in the substrate diffuse outward into the coating and the beneficial element Al diffuses into the substrate under the chemical composition gradient, the amounts of β phase are changed into the γ′ phase at the interface of the outer layer and inner layer. Due to the different solutions of the refractory elements in β and γ′ phases, the Cr(W) rich phases dissolve gradually in the inner layer. At the same time, the Cr(W) rich phases aggregate together and grow into larger particle sizes than before oxidation, which has been observed in our previous papers [18,22]. In addition, due to the mutual diffusion between the substrate and coating, there is some grey granular phase rich in Cr and bright needle-like phase rich in Cr and W formed in the substrate beneath the inner layer, which is called the secondary reaction zone. The grey granular Cr rich phase and needle-like Cr/W rich phase have been demonstrated to be the $M_{23}C_6$ and μ phase, respectively, by Liu et al. [18]. The μ phase is detrimental to the mechanical properties of the alloy, since it induces cracks in the substrate.

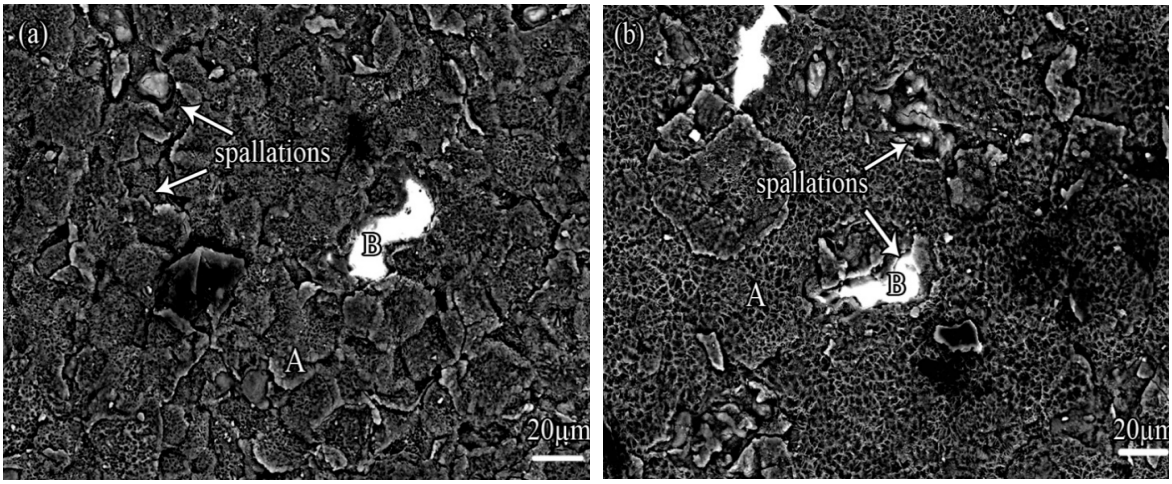

Figure 7. Surface morphologies of the coatings after oxidation at 1100 °C for 320 h: (**a**) PtAl and (**b**) PtSiAl.

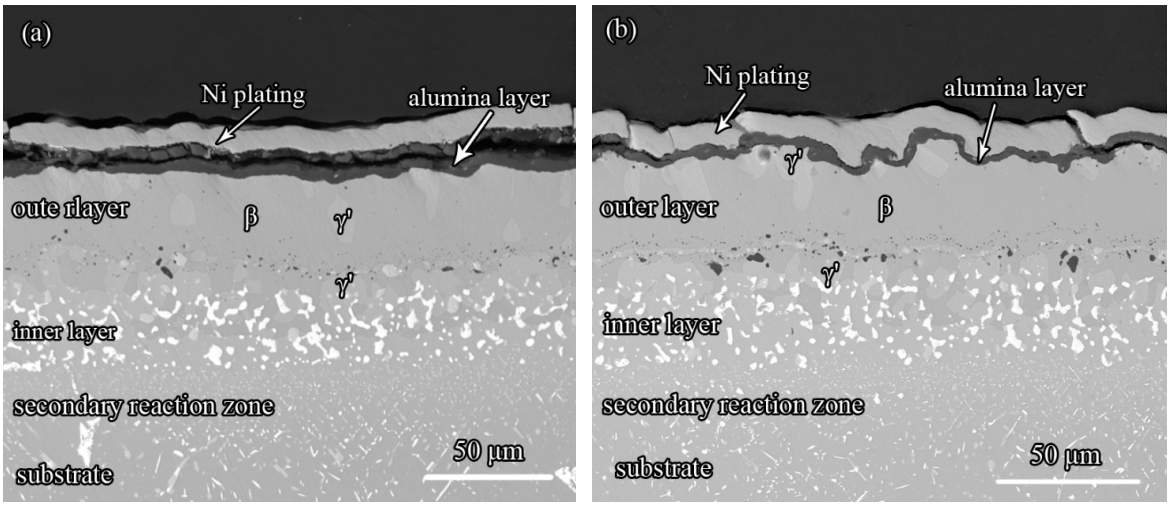

Figure 8. Cross-sectional morphologies of the coatings after oxidation at 1100 °C for 320 h: (**a**) PtAl and (**b**) PtSiAl.

3.4. The Effect of Si on the Microstructure and Oxidation Resistance of the Pt Modified Aluminide Coating

To analysis the Si effect on the microstructure of the PtSiAl coating, the element distributions of the coating from the surface to substrate are detected by SEM, as shown in Figure 9. The purple line represents the Si content in the coating. It can be seen that the Si content in the outer layer is lower than that in the inner layer. As mentioned above, the average Si content in the outer layer is about 0.7 at.%, which is much lower than its solubility in NiAl phase (2–4 at.%) [23], revealing that Si is dissolved in the (Ni, Pt)Al phase, which is consistent with the XRD pattern (Figure 1) where no silicide is detected. The dissolution of Si is beneficial for retarding the formation of the metastable phase $PtAl_2$, which might be attributed to the fact that Si has a very low diffusion rate in the $PtAl_2$ phase [17] and the deposition of Si might hinder the nucleation of the $PtAl_2$ phase. In addition, there are less voids formed on the surface of the Si doped Pt modified aluminide coating than the Pt modified aluminide coating. The generation of voids is mainly resultant from the unequal diffusion fluxes of the Ni and Al elements during the silico-aluminizing process. The addition of Si into the coating might increase the outward diffusion of Ni since the Ni content in the outer layer of the PtSiAl coating is a little higher than that in the PtAl coating and Si could occupy the vacancies in the coating, resulting in the decrease of voids. The Si content in the inter diffusion zone fluctuates strongly, which indicates that Si distributes unevenly in this zone. It is reported that Si has a high affinity with the refractory elements, especially the Cr element, forming silicide in the substrate [1,17]. In the inner layer, the contents of the Cr and W elements are high, which could promote the precipitation of silicide. It is worth noting that the Si content is much lower than the Al content in the PtSiAl coating, since the equilibrium vapor pressure of AlF which is responsible for depositing Al is much higher than that of SiF_y used to deposit Si in the chamber furnace at high temperature, when the fluoride is used as an activator [24]. Additionally, the deposition rate of the element is primarily dependent upon the quantity of the active halide. Thus, more Al element is deposited in the PtSiAl coating during the deposition process.

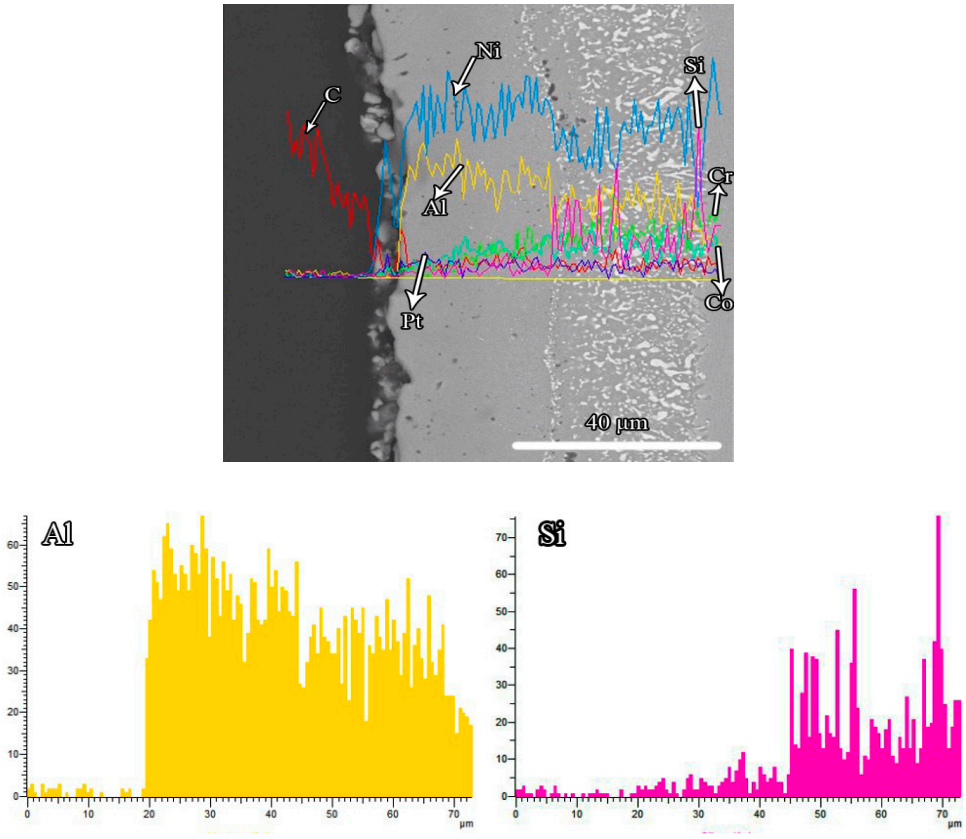

Figure 9. *Cont.*

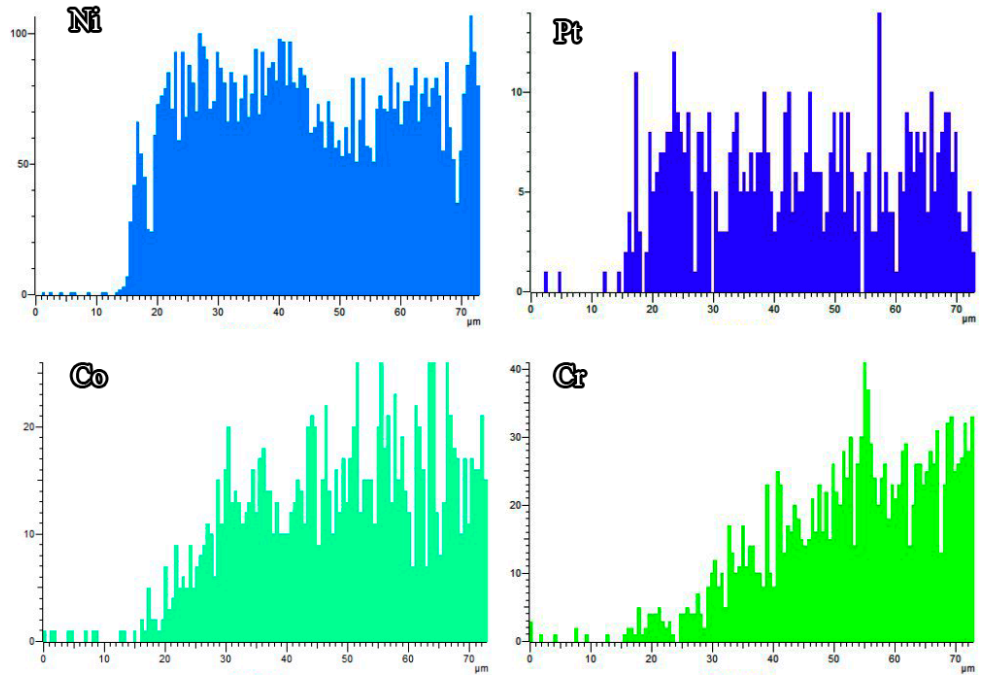

Figure 9. The line scanning image of the PtSiAl coating from outside to the inner layer by SEM.

The effect of Si on the properties of the simple aluminide coating has been reported by some researchers, but there has been no report about how Si influences the properties of the Pt modified aluminide coating up to now. According to the kinetic curves (Figure 4) and cross-sectional morphologies (Figure 8) of the PtAl and PtSiAl coatings, the PtSiAl coating possesses a lower mass gain than the PtAl coating and the thickness of the alumina layer formed on the surface of the PtSiAl coating is thinner. It can be concluded that the addition of Si could reduce the oxidation rate of the Pt modified aluminide coating, since Si could cut down the transient oxidation stage and promote the formation of α-Al_2O_3 [25,26]. It has been reported that the growth rate of the meta-stable θ alumina is higher than that of the stable α-alumina [27,28]. Meanwhile, the quick formation of an α-Al_2O_3 scale could retard the rapid diffusion of oxygen into the aluminide layer and lower the oxidation rate. On the other hand, Si forms silicide with the refractory elements Cr, W, and Mo in the inter-diffusion zone, which favors the inhibition of the outward diffusion of these refractory elements towards the outer layer [29]. In Figure 7, the W content on the surface (both area A and B) of the PtSiAl coating is less than that on the surface of the PtAl coating after oxidation for 320 h, which is beneficial for decreasing the generation of detrimental volatile oxide MoO_3 or WO_3. Consequently, the addition of Si into the Pt modified aluminide coating is beneficial for enhancing the oxidation resistance of the coating.

4. Conclusions

A Si doped Pt modified aluminide coating has been prepared by a combined method of electroplating and the vapour chemical deposition method. Like the Pt modified aluminide coating, the Si doped Pt modified aluminide coating possesses a two-layer structure. The outer layer consists of singular β-(Ni, Pt)Al phase. The average content of Si in the outer layer is about 0.7 at.% and no compound of Si or $PtAl_2$ phase is detected by XRD, revealing that Si is dissolved in the β-(Ni, Pt)Al phase in the outer layer and it might play a role in retarding the formation of $PtAl_2$ phase. Si is mainly concentrated in the inter-diffusion zone and it could form silicide with refractory elements like Cr and W.

The addition of Si into the Pt modified aluminide coating could enhance the oxidation resistance of the coating. On one hand, it could reduce voids on the coating surface and promote the exclusive

oxidation of α-Al_2O_3, leading to a lower oxidation rate. On the other hand, the silicide formed in the inter-diffusion zone could retard the diffusion of the refractory elements such as Cr, W, etc., which is beneficial for decreasing the formation of detrimental volatile phases in the coating.

Author Contributions: Conceptualization, H.Y. and Q.F.; Methodology, H.Y. and Q.F.; Validation, H.Y. and Q.F.; Formal Analysis, H.Y., Q.F., and T.W.; Investigation, Q.F.; Resources, H.Y., Q.F., T.W. and Y.L.; Data Curation, H.Y. and Q.F.; Writing-Original Draft Preparation, Q.F.; Writing-Review & Editing, Q.F.; Visualization, Q.F.; Supervision, Q.F.; Project Administration, Q.F.; Funding Acquisition, H.Y., Q.F., T.W. and Y.L.

Funding: This work was funded by the National Nature Science Foundation of China (Grant Nos. 51501130 and 51301181), Innovation Team Training Plan of Tianjin Universities and Colleges (Grant No. TD13-5096), and the Research Development Foundation of Tianjin University of Technology and Education (KJY14-03).

Conflicts of Interest: The authors declare no conflict of interest.

References

1. He, J.; Luan, Y.; Guo, H.; Peng, H.; Zhang, Y.; Zhang, T.; Gong, S. The role of Cr and Si in affecting high-temperature oxidation behaviour of minor Dy doped NiAl alloys. *Corros. Sci.* **2013**, *77*, 322–333. [CrossRef]
2. Marino, K.A.; Carter, E.A. Ni and Al diffusion in Ni-rich NiAl and the effect of Pt additions. *Intermetallics* **2010**, *18*, 1470–1479. [CrossRef]
3. Liu, R.D.; Jiang, S.M.; Yu, H.J.; Gong, J.; Sun, C. Preparation and hot corrosion behaviour of Pt modified AlSiY coating on a Ni-based superalloy. *Corros. Sci.* **2016**, *104*, 162–172. [CrossRef]
4. Svensson, H.; Christensen, M.; Knutsson, P.; Wahnström, G.; Stiller, K. Influence of Pt on the metal–oxide interface during high temperature oxidation of NiAl bulk materials. *Corros. Sci.* **2009**, *51*, 539–546. [CrossRef]
5. Chen, Y.; Zhao, X.; Bai, M.; Chandio, A.; Wu, R.; Xiao, P. Effect of platinum addition on oxidation behaviour of γ/γ' nickel aluminide. *Acta Mater.* **2015**, *86*, 319–330. [CrossRef]
6. Pomeroy, M.J. Coatings for gas turbine materials and long term stability issues. *Mater. Des.* **2005**, *26*, 223–231. [CrossRef]
7. Zhou, Z.; Peng, H.; Zhang, L.; Guo, H.; Gong, S. Microstructure and cyclic oxidation behaviour of low-Pt/Dy co-doped β-NiAl coatings on single crystal (SC) superalloy. *Surf. Coat. Technol.* **2016**, *304*, 108–116. [CrossRef]
8. Yang, Y.F.; Jiang, C.Y.; Yao, H.R.; Bao, Z.B.; Zhu, S.L.; Wang, F.H. Preparation and enhanced oxidation performance of a Hf-doped single-phase Pt-modified aluminide coating. *Corros. Sci.* **2016**, *113*, 17–25. [CrossRef]
9. Song, Y.; Murakami, H.; Zhou, C. Cyclic Corrosion Behavior of Pt/Ru-Modified Bond Coatings Exposed to NaCl Plus Water Vapor at 1050 °C. *J. Mater. Sci. Technol.* **2010**, *26*, 217–222. [CrossRef]
10. Song, Y.; Murakami, H.; Zhou, C. Cyclic-Oxidation Behavior of Multilayered Pt/Ru-Modified Aluminide Coating. *J. Mater. Sci. Technol.* **2011**, *27*, 280–288. [CrossRef]
11. Hong, S.J.; Hwang, G.H.; Han, W.K.; Lee, K.S.; Kang, S.G. Effect of zirconium addition on cyclic oxidation behavior of platinum-modified aluminide coating on nickel-based superalloy. *Intermetallics* **2010**, *18*, 864–870. [CrossRef]
12. Firouzi, A.; Shirvani, K. The structure and high temperature corrosion performance of medium-thickness aluminide coatings on nickel-based superalloy GTD-111. *Corros. Sci.* **2010**, *52*, 3579–3585. [CrossRef]
13. Shirvani, K.; Mastali, S.; Rashidghamat, A.; Abdollahpour, H. The effect of silicon on thermal shock performance of aluminide-thermal barrier coatings. *Corros. Sci.* **2013**, *75*, 142–147. [CrossRef]
14. Taniguchi, S.; Uesaki, K.; Zhu, Y.C.; Matsumoto, Y.; Shibata, T. Influence of implantation of Al, Si, Cr or Mo ions on the oxidation behaviour of TiAl under thermal cycle conditions. *Mater. Sci. Eng. A* **1999**, *266*, 267–275. [CrossRef]
15. Clemens, D.; Vosberg, V.; Hobbs, L.W.; Breuer, U.; Quadakkers, W.J.; Nickel, H. TEM and SNMS studies of protective alumina scales on NiCrAlY-alloys. *Fresenius J. Anal. Chem.* **1996**, *355*, 703–706. [CrossRef] [PubMed]
16. He, H.; Liu, Z.; Wang, W.; Zhou, C. Microstructure and hot corrosion behavior of Co–Si modified aluminide coating on nickel based superalloys. *Corros. Sci.* **2015**, *100*, 466–473. [CrossRef]
17. Azarmehr, S.A.; Shirvani, K.; Schütze, M.; Galetz, M. Microstructural evolution of silicon-platinum modified aluminide coatings on superalloy GTD-111. *Surf. Coat. Technol.* **2017**, *321*, 455–463. [CrossRef]

18. Fan, Q.X.; Peng, X.; Yu, H.J.; Jiang, S.M.; Gong, J.; Sun, C. The isothermal and cyclic oxidation behaviour of two Co modified aluminide coatings at high temperature. *Corros. Sci.* **2014**, *84*, 42–53. [CrossRef]
19. Liu, R.D.; Jiang, S.M.; Guo, C.Q.; Gong, J.; Sun, C. The alumina scale growth and interdiffusion behaviour of Pt modified AlSiY coating during cyclic oxidation. *Corros. Sci.* **2017**, *120*, 121–129. [CrossRef]
20. Hong, S.J.; Hwang, G.H.; Han, W.K.; Kang, S.G. The effect of Pt contents on the surface morphologies of Pt-modified aluminide coating. *Surf. Coat. Technol.* **2009**, *203*, 3066–3071. [CrossRef]
21. Hong, S.J.; Hwang, G.H.; Han, W.K.; Kang, S.G. Cyclic oxidation of Pt/Pd-modified aluminide coating on a nickel-based superalloy at 1150 °C. *Intermetallics* **2009**, *17*, 381–386. [CrossRef]
22. Fan, Q.X.; Jiang, S.M.; Wu, D.L.; Gong, J.; Sun, C. Preparation and hot corrosion behaviour of two Co modified NiAl coatings on a Ni-based superalloy. *Corros. Sci.* **2013**, *76*, 373–381. [CrossRef]
23. Shirvani, K.; Saremi, M.; Yamaoto, Y. The approaches to thin film preparation and TEM observations on slurry Si-modified aluminide coatings. *Mater. Corros.* **2006**, *57*, 182–184. [CrossRef]
24. Xiang, Z.D.; Datta, P.K. Codeposition of Al and Si on nickel base superalloys by pack cementation process. *Mater. Sci. Eng. A* **2003**, *356*, 136–144. [CrossRef]
25. Fu, C.; Kong, W.K.; Cao, G.H. Microstructure and oxidation behavior of Al+Si co-deposited coatings on nickel-based superalloys. *Surf. Coat. Technol.* **2014**, *258*, 347–352. [CrossRef]
26. Dai, P.; Wu, Q.; Ma, Y.; Li, S.; Gong, S. The effect of silicon on the oxidation behavior of NiAlHf coating system. *Appl. Surf. Sci.* **2013**, *271*, 311–316. [CrossRef]
27. Hamadi, S.; Bacos, M.P.; Poulain, M.; Seyeux, A.; Maurice, V.; Marcus, P. Oxidation resistance of a Zr-doped NiAl coating thermochemically deposited on a nickel-based superalloy. *Surf. Coat. Technol.* **2009**, *204*, 756–760. [CrossRef]
28. Zhou, Y.; Zhao, X.; Zhao, C.; Hao, W.; Wang, X.; Xiao, P. The oxidation performance for Zr-doped nickel aluminide coating by composite electrodepositing and pack cementation. *Corros. Sci.* **2017**, *123*, 103–115. [CrossRef]
29. Gong, S.; Zhang, D.; Xu, H.; Han, Y. Thermal barrier coatings with two layer bond coat on intermetallic compound Ni_3Al based alloy. *Intermetallics* **2005**, *13*, 295–299. [CrossRef]